HELDA
HELSINGIN YLIOPISTO
HELSINGFORS UNIVERSITET
UNIVERSITY OF HELSINKI

UNIVERSITY OF HELSINKI

https://helda.helsinki.fi

Reconnection rates and X line motion at the magnetopause : Global 2D-3V hybrid-Vlasov simulation results

Hoilijoki, Sanni

2017-03

Hoilijoki , S , Ganse , U , Pfau-Kempf , Y , Cassak , P A , Walsh , B M , Hietala , H , von Alfthan , S & Palmroth , M 2017 , ' Reconnection rates and X line motion at the magnetopause : Global 2D-3V hybrid-Vlasov simulation results ' , Journal of geophysical research. Space physics , vol. 122 , no. 3 , pp. 2877-2888 . https://doi.org/10.1002/2016JA023709

http://hdl.handle.net/10138/224164
https://doi.org/10.1002/2016JA023709

publishedVersion

Downloaded from Helda, University of Helsinki institutional repository.

This is an electronic reprint of the original article.

This reprint may differ from the original in pagination and typographic detail.

Please cite the original version.

AGU PUBLICATIONS

JGR

Journal of Geophysical Research: Space Physics

RESEARCH ARTICLE
10.1002/2016JA023709

Reconnection rates and X line motion at the magnetopause: Global 2D-3V hybrid-Vlasov simulation results

Sanni Hoilijoki[1], Urs Ganse[1], Yann Pfau-Kempf[1], Paul A. Cassak[2], Brian M. Walsh[3], Heli Hietala[4], Sebastian von Alfthan[5], and Minna Palmroth[1,6]

[1]Department of Physics, University of Helsinki, Helsinki, Finland, [2]Department of Physics and Astronomy, West Virginia University, Morgantown, West Virginia, USA, [3]Mechanical Engineering and Center for Space Physics, Boston University, Boston, Massachusetts, USA, [4]Department of Earth, Planetary and Space Sciences, University of California, Los Angeles, California, USA, [5]CSC-IT Center for Science Ltd., Espoo, Finland, [6]Finnish Meteorological Institute, Helsinki, Finland

Abstract We present results from a first study of the local reconnection rate and reconnection site motion in a 2D-3V global magnetospheric self-consistent hybrid-Vlasov simulation with due southward interplanetary magnetic field. We observe magnetic reconnection at multiple locations at the dayside magnetopause and the existence of magnetic islands, which are the 2-D representations of flux transfer events. The reconnection locations (the X lines) propagate over significant distances along the magnetopause, and reconnection does not reach a steady state. We calculate the reconnection rate at the location of the X lines and find a good correlation with an analytical model of local 2-D asymmetric reconnection. We find that despite the solar wind conditions being constant, the reconnection rate and location of the X lines are highly variable. These variations are caused by magnetosheath fluctuations, the effects of neighboring X lines, and the motion of passing magnetic islands.

Key Points:
- We study dayside magnetic reconnection in a global magnetospheric self-consistent hybrid-Vlasov simulation
- Flux transfer events are always present and the dayside X lines are influenced both by magnetosheath properties and other reconnection sites
- The local reconnection rate correlates well with an analytic prediction

Supporting Information:
- Supporting Information S1
- Movie S1

Correspondence to:
S. Hoilijoki,
sanni.hoilijoki@fmi.fi

Citation:
Hoilijoki, S., U. Ganse, Y. Pfau-Kempf, P. A. Cassak, B. M. Walsh, H. Hietala, S. von Alfthan, and M. Palmroth (2017), Reconnection rates and X line motion at the magnetopause: Global 2D-3V hybrid-Vlasov simulation results, *J. Geophys. Res. Space Physics*, *122*, 2877–2888, doi:10.1002/2016JA023709.

Received 23 NOV 2016
Accepted 12 FEB 2017
Accepted article online 17 FEB 2017
Published online 3 MAR 2017

©2017. American Geophysical Union. All Rights Reserved.

1. Introduction

Magnetic reconnection takes place when magnetic field with a component that changes direction undergoes a change in topology [*Dungey*, 1953]. At the dayside magnetopause of the Earth's magnetosphere during southward interplanetary magnetic field (IMF), solar wind magnetic field lines reconnect with the terrestrial field. The resulting field lines advect tailward with the solar wind flow allowing mixing between magnetospheric and magnetosheath plasmas [*Dungey*, 1961]. Much has been learned about reconnection at the dayside magnetopause, but there remain a number of open questions. Here we address the following—is reconnection laminar or bursty for steady solar wind conditions, how does structure in the magnetosheath impact dayside reconnection, what controls the reconnection rate at the dayside, and what controls the motion of flux transfer events when reconnection is bursty. A lot of work has been done on these questions using global magnetospheric simulations with magnetohydrodynamic (MHD) models, but as we argue below, these questions require a kinetic approach. We address these questions using global magnetospheric simulations with a hybrid code using the Vlasov description for ions and a fluid model for electrons.

Difficulty in predicting the local reconnection rate at the dayside magnetopause is due to the fact that the reconnecting plasmas on the two sides of the reconnecting current sheet are dissimilar: the process is asymmetric; density is usually higher and magnetic field lower in the magnetosheath than in the magnetosphere. The reconnection rate, a local measure of the efficiency of the reconnection process, can be determined by the amount of magnetic flux reconnected. The reconnection rate in two-dimensional (2-D) asymmetric reconnection has been found to depend on the plasma parameters in both inflow regions [*Cassak and Shay*, 2007], but this study employed a rectangular geometry, so it is not clear whether the theory applies to the magnetosphere. Using a global magnetohydrodynamic (MHD) simulation, both *Borovsky et al.* [2008] and *Ouellette et al.* [2014] have found that the dayside reconnection rate agrees with the analytical equations derived by *Cassak and Shay* [2007] during southward IMF, indicating that the reconnection rate at the magnetopause is driven by local plasma conditions. *Komar and Cassak* [2016] tested the theory against the local reconnection rate in global resistive MHD simulations using oblique IMF directions. They found very good agreement in the scaling sense, with excellent absolute results for southward IMF and an increasing multiplicative offset for decreasing clock angle. However, these tests employed an MHD model. Even in the slab geometry, MHD has limitations

for studying asymmetric reconnection, because the plasma mixing in the exhaust is not described realistically [*Cassak and Shay*, 2009; *Birn et al.*, 2010; *Ouellette et al.*, 2014]. This suggests that a kinetic simulation is better to test the reconnection model.

Reconnection at the magnetopause can lead to the development of flux transfer events (FTEs) that are usually observed as bipolar variations in the magnetic field component normal to the local magnetopause [*Russell and Elphic*, 1978]. The structures are typically observed during southward IMF orientations [e.g., *Kawano and Russell*, 1997; *Wang et al.*, 2005, 2006; *Fear et al.*, 2009, 2010; *Eastwood et al.*, 2012]. In some observational studies, FTEs have also been found to occur as nearly periodic phenomena with average spacing of 8 min [*Rijnbeek et al.*, 1984]. Different theories about the formation mechanisms of FTEs include temporally varying single X line reconnection [*Scholer*, 1988; *Southwood et al.*, 1988] and multiple X line reconnection [*Lee and Fu*, 1985].

Whether the dayside magnetopause reconnection is manifested in single or multiple X line configurations, i.e., whether it is steady or patchy under different solar wind conditions, is not yet well known. Our understanding is limited by the localized nature of individual spacecraft measurements and because most numerical studies used MHD models, which does not describe reconnection physics well in the nearly collisionless magnetosphere. Multiple X line reconnection and/or formation of FTEs has been simulated using global MHD models [e.g., *Fedder et al.*, 2002; *Raeder*, 2006; *Dorelli and Bhattacharjee*, 2009]. *Shi et al.* [1988] found using a 2-D MHD simulation that if the magnetic Reynolds number is high, multiple X lines exist simultaneously, while with a low magnetic Reynolds number, reconnection occurs on a single X line. *Raeder* [2006] reported multiple X lines and formation of FTEs in an MHD simulation during southward IMF with large dipole tilt angle, but without the dipole tilt, the reconnection took place only at one steady X line. However, using a resistive MHD simulation, *Dorelli and Bhattacharjee* [2009] showed that FTEs can also form without a dipole tilt. Yet MHD simulations do not include ion scale physics and therefore are not able to describe, for example, the microphysics of reconnection and foreshock and magnetosheath waves unlike hybrid-PIC and hybrid-Vlasov simulations [e.g., *Blanco-Cano et al.*, 2006, 2009; *Karimabadi et al.*, 2014; *Kempf et al.*, 2015]. Previous studies employing 2-D hybrid-PIC simulations have shown the formation of multiple X lines and FTE with southward IMF and no dipole tilt [*Karimabadi et al.*, 2006; *Omidi and Sibeck*, 2007; *Sibeck and Omidi*, 2012]. Similar results have also been found with 3-D global hybrid-PIC simulations [*Karimabadi et al.*, 2006; *Tan et al.*, 2011]. Variations of the local reconnection rate at the multiple X lines and the plasma parameters that affect the reconnection rate have not been investigated before using a global hybrid simulation.

The motion of X lines has been studied both theoretically and using spacecraft measurements. In a theoretical consideration, *Cowley and Owen* [1989] suggested that the magnetosheath flows affect the motion of newly reconnected flux tubes, which may also be manifested in the motion of the X line itself. *Doss et al.* [2015] found that X lines advect during asymmetric reconnection if there is a velocity shear between the upstream and downstream region. However, the motion of X lines and the parameters that affect it have not been studied in global ion kinetic models. In a global 2-D setup using hybrid-PIC simulations, *Sibeck and Omidi* [2012] studied the formation and propagation of FTEs. In the simulation, FTEs formed between two X lines remaining almost steadily at the subsolar point before they started moving poleward. Some of the structures started moving initially toward the equator before coalescing with other FTEs and escaping poleward.

In this paper we present the first results on the variations of the local reconnection rate and X line motion on the magnetopause as manifested in a global 2D-3V kinetic simulation describing the solar wind-magnetosphere interaction self-consistently. We locate the X lines at the dayside magnetopause and calculate reconnection rates at these points. We find a general agreement with the analytical model derived by *Cassak and Shay* [2007]. We also demonstrate that reconnection takes place continuously at the dayside magnetopause but the location of the dominant X line can move significantly over time even though the solar wind is kept constant and the IMF direction is maintained as due south.

2. Vlasiator Simulation

We use the hybrid-Vlasov code Vlasiator (http://vlasiator.fmi.fi), which is a global simulation code modeling the Earth's magnetosphere using a kinetic physical description [*von Alfthan et al.*, 2014]. Ions are treated as 3-D velocity distribution functions propagated by the Vlasov equation, while electrons are a charge-neutralizing fluid. For a more detailed technical description of Vlasiator, see *von Alfthan et al.* [2014] and *Kempf et al.* [2015].

However, note that those papers did not include the Hall term in the generalized Ohm's law, which was added in the version described in *Palmroth et al.* [2015]; we use the version with the Hall term in this study.

The simulation discussed in this paper is carried out in the Geocentric Solar Ecliptic (GSE) polar *xz* plane in a 2-D setup in ordinary space, while the velocity space in each cell is 3-D. A 2-D line dipole corresponding to the Earth's dipole strength is applied as in *Daldorff et al.* [2014]. While the simulation box extends from $x = -94\ R_E$ to $+48\ R_E$ and in the *z* direction to $\pm 56\ R_E$, we concentrate in this paper only on dayside phenomena. The solar wind with constant magnetic field and Maxwellian velocity distributions flows in from the sunward wall while a copy condition is applied at the other three boundaries; i.e., at the boundary cells the velocity distribution function and magnetic field are copied from the nearest spatial cell that is inside the simulation domain. The resolution is uniform in the entire simulation domain: 300 km in ordinary space and 30 km/s in velocity space. The IMF is purely southward with a magnitude of 5 nT. The number density in the solar wind is $n = 1\ \mathrm{cm}^{-3}$ and the velocity is −750 km/s along the *x* axis. The proton temperature in the solar wind plasma is 0.5 MK. Initially, the whole simulation domain includes constant density and bulk velocity set to the same values as in solar wind and the dipole magnetic field. The magnetosphere, magnetosheath, and the bow shock form self-consistently as the inflowing solar wind interacts with the dipole field. We consider that the dayside magnetosheath and magnetopause are initialized when the inflowing solar wind with southward IMF has crossed the magnetosheath and has reached the subsolar point of the dayside magnetopause. This happens approximately at 800 s simulated time.

3. Results

3.1. Magnetosheath

The results show a number of dynamic kinetic features. Figure 1a shows the ratio of plasma pressure to the magnetic pressure (plasma β) on the dayside magnetosheath and magnetopause (at $t = 1800$ s simulated time) showing large β variations. Waves in the magnetosheath in our simulation have an anticorrelation between magnetic field and density fluctuations as shown in Figure 1c, suggesting that these waves could be mirror mode waves. We test the magnetosheath waves against the mirror mode criteria as has been done previously in the equatorial plane simulation by *Hoilijoki et al.* [2016]. In this study we used the same criteria as those used by *Genot* [2009]. First, mirror mode waves are known to have large amplitude [e.g., *Tatrallyay*, 2005; *Genot*, 2009] and, therefore, we require the standard deviation of the fluctuations of the magnetic field magnitude to be larger than 10%. The linear polarization of waves is checked by calculating the angle between the background magnetic field and the maximum variance direction, which is required to be smaller than 20° [*Genot*, 2009; *Genot*, 2011]. The waves in the magnetosheath, from the central sheath to the vicinity of the magnetopause near the equatorial region fulfill these criteria. The mirror mode waves advect toward the dayside magnetopause where reconnection takes place at many X lines simultaneously.

3.2. Motion of X Lines

Multiple magnetic islands, 2-D representations of FTEs, are forming and evolving at the magnetopause throughout the simulation after the dayside magnetosphere has been initialized. Figure 1b shows the *z* component of the plasma velocity v_z at time 1800 s with magnetic field lines shown in black. At that time, the strongest X line, where the plasma flow along the magnetopause diverts between north and south, is located close to $z = -0.8\ R_E$. Just north of this X line, a large FTE is forming. In addition, multiple other X lines are present simultaneously, but the reconnection at these X lines is not strong enough to divert the plasma flow northward and southward.

We determine the locations of magnetic reconnection points and centers of magnetic islands (X and O points) by finding the local saddle points and maxima, respectively, of the magnetic flux function Ψ that is calculated from $\mathbf{B} = \hat{\mathbf{y}} \times \nabla\Psi$ by integrating $\mathbf{B}$ over the whole simulation domain [e.g., *Yeates and Hornig*, 2011]; magnetic field lines are lines of constant Ψ. The raw flux function is smoothed by convolution with a 5×5 box kernel to decrease the number of points yielded by this sensitive method. Figure 2 indicates the *z* coordinate of the magnetopause X points (black) and O points (yellow) as a function of time. The background is color coded with the *z* component of the bulk velocity V_z measured at the magnetopause and plotted as a function of *z* and time. This plot depicts the location of the strongest X line. This point moves between $z = \pm 3\ R_E$, and occasionally there are two stronger X lines that are able to divert the flow. Figure 2 visualizes how both the X lines and magnetic islands move along the magnetopause. To illustrate the motion of the X lines and magnetic islands, we present a movie of V_z in the dayside magnetosheath (see Movie S1 in the supporting information).

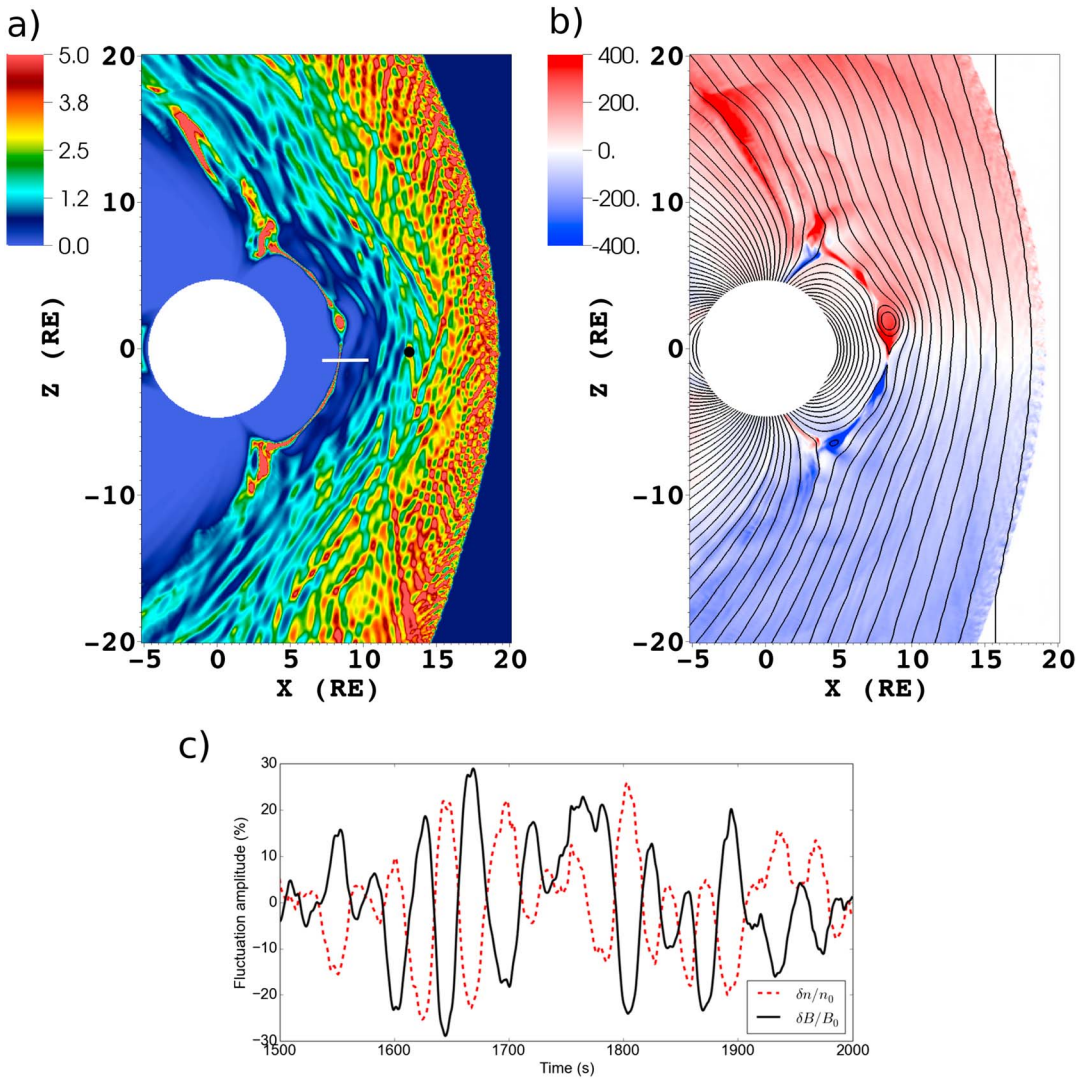

Figure 1. (a) Plasma β and (b) V_z in km/s at time $t = 1800$ s. The black lines show the magnetic field lines. The white line depicts the cut through the magnetopause discussed in Figure 7. Distances are given in R_E. (c) Magnetic field strength (black solid) and density (red dashed) fluctuations from the virtual spacecraft location indicated with the black dot in Figure 1a.

Instead of traveling from the subsolar point toward the poles in the same direction with the magnetosheath plasma flow, some of the X lines and FTEs propagate also toward the subsolar point, change direction, and decelerate or accelerate similar to what was previously reported by *Sibeck and Omidi* [2012]. The motion of the X lines seems to be dependent not only on magnetosheath flow but also on the propagation and the outflow velocities of nearby X lines. The dayside reconnection does not attain a steady state during the simulation even though solar wind parameters are kept constant.

3.3. Reconnection Rate at the X Lines

Figure 3 shows the location of the X lines and O points as in Figure 2, but now the X line markers are color coded with the local reconnection rate, i.e., the out-of-plane electric field E_y at the X line. The reconnection rate is positive when the reconnection takes place between magnetospheric and solar wind magnetic field lines. However, sometimes in Figure 3 the reconnection rate switches from positive to negative. The negative values indicate reconnection between magnetic field lines of newly formed magnetic islands. Coalescing of two magnetic islands is illustrated in Figure 4, which shows a region from the dayside magnetopause at four different time steps. Figure 4a, at $t = 1650$ s, shows the formation of a new magnetic island (labeled as FTE 1 in Figures 3 and 4) near $z = -1\ R_E$ between two X lines (labeled as X1 and X2). At this time the reconnection rate

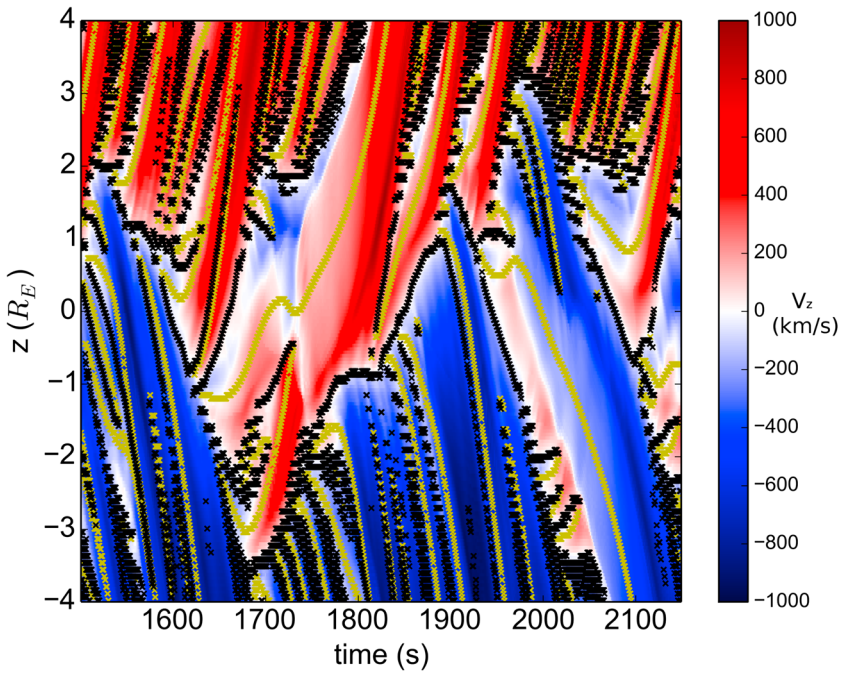

Figure 2. Location of X points (black) and O points (yellow) at the magnetopause and the color coding shows the z component of the ion bulk velocity V_z (km/s) at the magnetopause over time.

at these two X lines is positive. In Figures 4b and 4c two magnetic islands, the one forming in Figure 4a located now at the subsolar point (FTE 1) and another one coming from the south (FTE 2), coalesce. The reconnection rate at the X line between these two islands (X2) turns negative for about 15 s, and finally, the X line disappears as seen also in Figure 3. In Figure 4d at time $t = 1800$ s the large FTE formed by multiple coalesced magnetic islands accelerates toward the northern cusp.

3.4. Comparison With Analytical Prediction

We calculate the reconnection rate analytically using the *Cassak and Shay* [2007] formula for all X lines between $z = \pm 4R_E$. The reconnection rate E_{pred} is given as a function of the upstream magnetic field magnitude B, upstream mass density ρ, and inflow velocity v:

$$E_{\text{pred}} \sim V_{\text{AH}} \left(\frac{B_1 B_2}{B_1 + B_2} \right) \frac{2\delta}{L} = \frac{B_1 B_2 (\rho_1 v_1 + \rho_2 v_2)}{\rho_1 B_2 + \rho_2 B_1}, \tag{1}$$

where δ/L is the aspect ratio of the dissipation region, δ is the half width, and L the half length of the reconnection dissipation region. Subscript 1 stands for the values on the magnetospheric side of the X line and subscript 2 stands for the magnetosheath values. For the reconnecting magnetic field values, B_1 and B_2, we use the tangential components corresponding to the L components in a boundary normal coordinate system (B_{L1} and B_{L2}) of the magnetic field in the inflow plasma regions. Variations in the out-of-plane component of the magnetic field (B_y) close to the magnetopause is less than 1% of the magnetic field on the simulation plane. For inflowing velocities, v_1 and v_2, we use the components normal to the local magnetopause (v_{N1} and v_{N2}). In writing the equality, we have eliminated δ/L using the expression from *Cassak and Shay* [2007] for mass conservation:

$$\delta/L \sim \frac{\rho_1 v_1 + \rho_2 v_2}{2\rho_{\text{out}} V_{\text{AH}}}, \tag{2}$$

where we use the following relations for the outflow density $\rho_{\text{out}} \sim (\rho_1 B_2 + \rho_2 B_1)/(B_1 + B_2)$ and the hybrid Alfvén velocity $V_{\text{AH}} \sim \sqrt{B_1 B_2 (B_1 + B_2)/\mu_0 (\rho_1 B_2 + \rho_2 B_1)}$.

To test whether equation (2) holds in the Vlasiator simulation, we consider the time period when one X line remains roughly at the same location for about 50 s from $t = 1775$ s to 1825 s at $z \approx -0.9\,R_E$ (black square box in Figure 2). Because the outflow is not symmetric, we generalize equation (2) by using

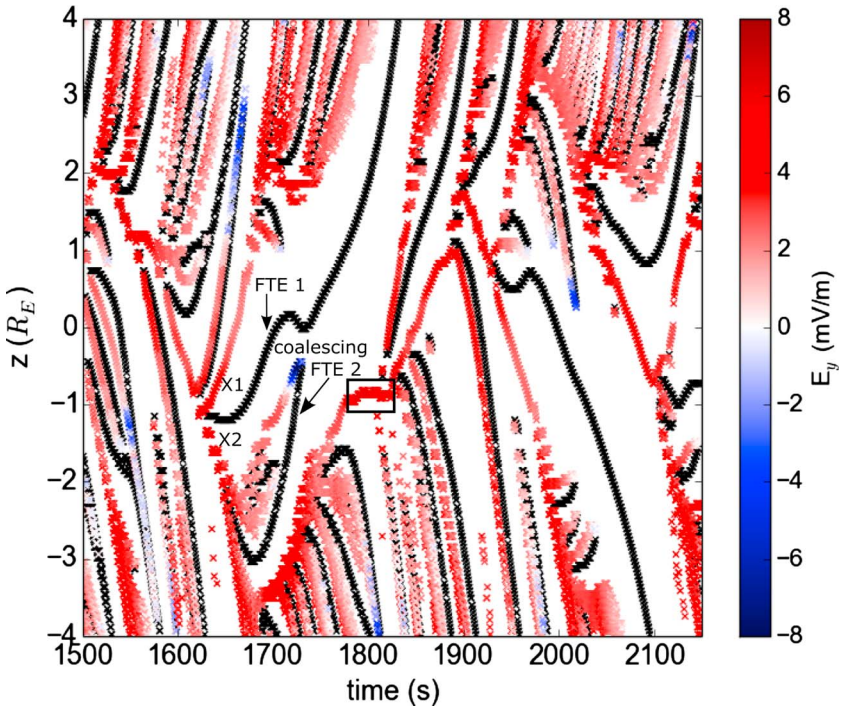

Figure 3. Location of X points (color coding) and O points (black) along the magnetopause *z* component. The color coding on the X point locations shows the measured local reconnection rate E_y. Labeled X lines and FTEs refer to section 3.2 and the rectangular box refers to sections 3.4 and 3.5.

$\rho_{out,S}v_{out,S} + \rho_{out,N}v_{out,N}$ instead of $2\rho_{out}V_{out}$ [*Murphy*, 2010]. Subscripts S and N stand for southward and northward outflow, respectively. Equation (2) becomes

$$\delta/L \sim \frac{\rho_1 v_1 + \rho_2 v_2}{\rho_{out,S}v_{out,S} + \rho_{out,N}v_{out,N}}. \quad (3)$$

As inflow parameters we use the same values that are used to calculate the reconnection rate prediction. The aspect ratio is obtained by calculating the square root of the ratio of the eigenvalues of the Hessian matrix at the X line as was done previously by *Servidio* [2009] and *Servidio*, [2010]: $\delta/L \sim \sqrt{\lambda_{min}/\lambda_{max}}$. The mean of the aspect ratio calculated over the considered time period yields 0.225. We estimate 2δ as one half the width of the J_y peak across the magnetopause and use the aspect ratio to calculate *L*. The outflow density and velocity are taken from a distance *L* from the X line location. The mean of the ratio of the inflowing and outflowing ρv is 0.234. The good match between these two values shows that equation (3) holds and can be used.

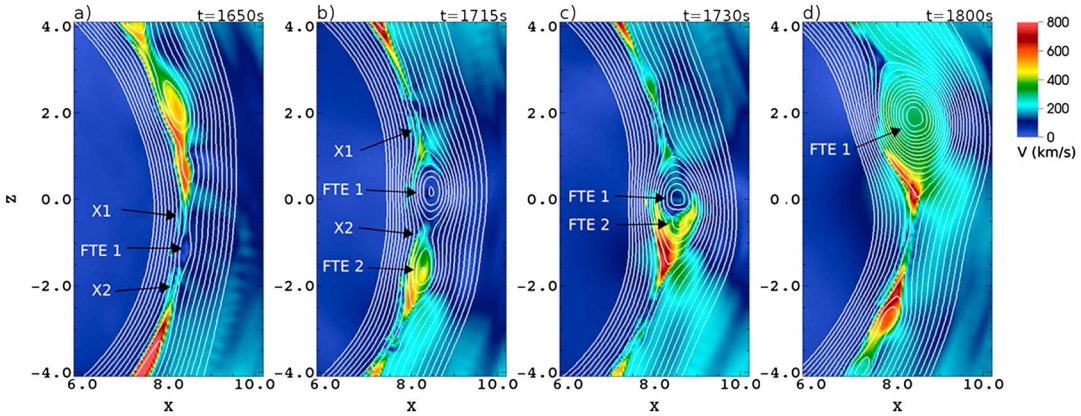

Figure 4. Cut from the dayside magnetopause at four different times (a) $t = 1650$ s, (b) $t = 1715$ s, (c) $t = 1730$ s, and (d) $t = 1800$ s. Color coding shows the magnitude of ion bulk velocity *v* (km/s), and the white lines depict the magnetic field lines.

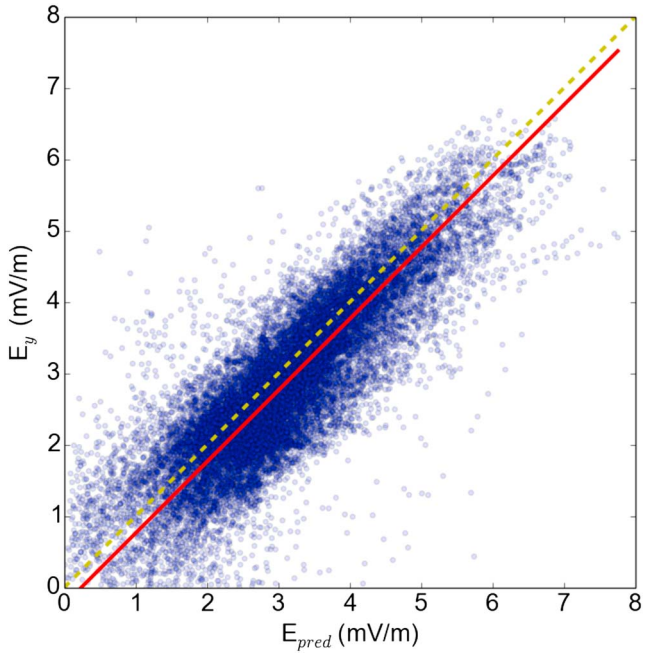

Figure 5. A scatterplot of the analytical prediction of the reconnection rate (*x* axis) and the measured reconnection rate (*y* axis). The yellow dashed line shows where these two would be equal, and the red solid line shows the orthogonal least squares fit $E_y = E_{\text{pred}} - 0.2$ mV/m.

All upstream parameters are taken from a distance of 1200 km ~0.19 R_E from the magnetopause, which corresponds approximately to nine ion inertial lengths of the magnetosheath, from the magnetopause along the magnetopause normal. This distance was chosen by (1) estimating where the current density J, B, and ρ level off after crossing the magnetopause, as well as, (2) testing which distance gives the best correlation and fit between the measured and predicted reconnection rate. Increasing or decreasing the distance worsen both the correlation coefficient and the least square orthogonal fit. The magnetopause location is determined by finding the B_z reversal, and the normals are calculated by forming a B spline fit of the magnetopause points and finding its normal directions.

In Figure 5 blue dots show the scatterplot between E_{pred} from equation (1) and the measured reconnection rate E_y. The yellow dashed line indicates where the two quantities are equal, and the red solid line is an orthogonal least squares fit that yields $E_y = E_{\text{pred}} - 0.2$ mV/m. The Pearson correlation coefficient between the measured and analytical prediction is 0.85. The results suggest that there is an overall good agreement with the predicted reconnection rate. However, there is some scatter in the data, so it is useful to investigate reasons why the match is not ideal.

One effect that could alter the reconnection rate is the presence of the magnetosheath flow, which was not included in the original model. It has been suggested that this flow can slow and even stop reconnection [e.g., *Mitchell Jr. and Kan*, 1978; *La BelleHamer et al.*, 1994; *Chen et al.*, 1997; *Li and Ma*, 2010; *Cassak and Otto*, 2011]. *Doss et al.* [2015] derived an analytical formula for the reconnection rate similarly as *Cassak and Shay* [2007] but for the case when there is an in-plane velocity shear between the inflowing regions. The correction term to the reconnection rate due to the shear is $1 - (v_{\text{shear}}/V_{\text{AH}})^2(4\rho_1 B_{L2}\rho_2 B_{L1})/(\rho_1 B_{L2} + \rho_2 B_{L1})^2$, where $v_{\text{shear}} = (v_{L1} - v_{L2})/2$ and the v_L components are in the outflow direction tangential to the magnetopause. For the present simulation, the effect of the correction term in the reconnection rate results is insignificant, yielding the same least squares fit and correlation coefficient when it is compared to the measured reconnection rate. This is very reasonable since we are only looking at X lines within 4 R_E of the subsolar point, so the flow shear is expected to be small. In addition, *Doss et al.* [2015] derived a formula for the drift speed of an isolated X line when there is a velocity shear: $v_{\text{drift}} \sim (\rho_1 B_{L2} v_{L1} + \rho_1 B_{L2} v_{L1})/(\rho_1 B_{L2} + \rho_2 B_{L1})$. In our simulation, the predicted v_{drift} for the X lines near the subsolar region often points in the opposite direction than the X lines are moving. This indicates that the other effects, such as outflow jets from nearby X lines, are more

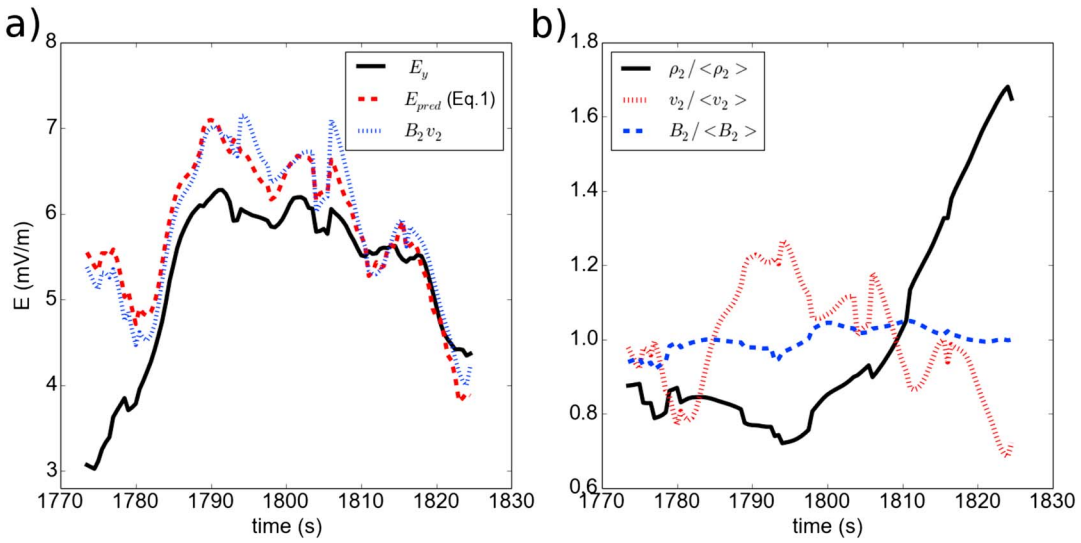

Figure 6. (a) Reconnection rate at the steady X line location (black line), corresponding rate given by equation (1) (red dashed line) and $B_2 v_2$ (blue dotted line), where the subscript 2 stands for magnetosheath inflow values. (b) Inflow density ρ_2 (black solid line), ion velocity v_2 (red dotted line), and tangential magnetic field component B_2 (blue dashed line) scaled by their time averages from the point where the magnetosheath values are read for equation (1).

important in defining the absolute X line motion near the subsolar region, consistent with the discussion in *Doss et al.* [2015].

Another reason for the differences between the measured and analytical reconnection rate is the possible inaccuracy of measuring the inflowing parameters as well as locating the X lines where the E_y is measured. The variance between the E_y values at the X line and its neighboring cells could be of the same order of magnitude than the difference between the measured and predicted rate. The fraction of points having a large difference between the measured and analytical reconnection rates increases slightly with latitude. At higher latitudes the X lines move faster, as does the magnetosheath plasma. The motion might cause inaccuracy in measuring the inflow values. Similarly, the choice of the distance, where the inflow values are taken, affects the correlation as mentioned above.

We do not assume that the aspect ratio δ/L is constant as has been done previously [e.g., *Borovsky et al.*, 2008], but we eliminated δ/L from equation (1) using the relation given by equation (2). Interestingly, when we test equation (1) with an assumed value of $\delta/L = 0.1$, we find that the Pearson correlation coefficient becomes significantly worse and is only 0.3. This implies that δ/L is not constant for our simulations. We suspect that the cause of the aspect ratio not being fixed at 0.1 is because we are not resolving the ion inertial scale with our computational grid, so the reconnection is likely more Sweet-Parker-like governed by grid scale diffusion, consistent with a varying aspect ratio.

3.5. Effect of Magnetosheath Parameters

To check whether magnetosheath waves have an effect on the reconnection rate, we consider again the X line that remains roughly at the same location for about 50 s from $t = 1775$ s to 1825 s at $z \approx -0.9\,R_E$ (black box in Figure 2). We plot the measured reconnection rate at the steady X line in Figure 6a (black), and in the same panel we plot the corresponding theoretical rate given by equation (1) (red dashed line). During this time period the Pearson correlation coefficient between these two is 0.73. The reconnection rate variations are dominated by the magnetosheath plasma parameters. Setting B_1, ρ_1, and v_1 (subscript 1 stands for magnetospheric values) to a constant value (mean over the considered time period), the reconnection rate prediction is almost identical than with varying magnetospheric inflow parameters. We also plot $B_{L2} v_2$ (subscript 2 = magnetosheath) in the same panel as the measured and predicted reconnection rate (Figure 6). The behavior of $B_{L2} v_2$ is almost the same as the reconnection rate calculated using all inflow values in equation (1). This is very reasonable, since $\mathbf{E} \sim -\mathbf{v} \times \mathbf{B}$ upstream of the reconnection site.

Next, we take a closer look at the terms in the numerator and denominator of equation (1). In the numerator, the term $\rho_2 v_2$ is larger than the magnetospheric $\rho_1 v_1$ due to the much higher density in the magnetosheath.

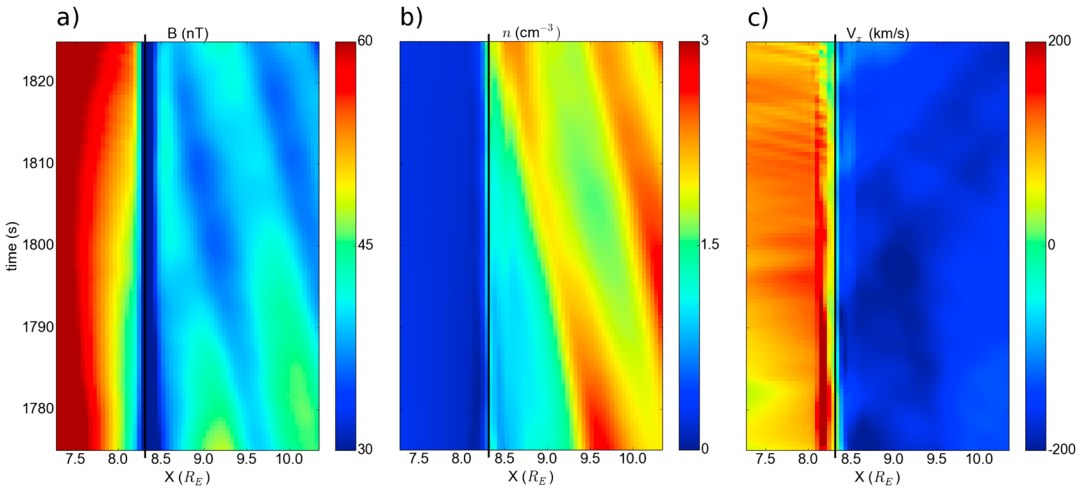

Figure 7. Stacked time series of (a) magnetic field magnitude, (b) number density, and (c) *x* component of the bulk velocity along the white line marked in Figure 1a. Time is on the vertical axis and *x* coordinate on the horizontal axis. The black line in each panel shows the location of the X line.

In the denominator the term with the magnetosheath density $\rho_2 B_{L1}$ is at least 10 times larger than $\rho_1 B_{L2}$ during the considered time period. Since $\rho_2 B_{L1}$ is in the denominator we calculate the Pearson correlation coefficient between the measured rate E_y and $(\rho_2 B_{L1})^{-1}$ and the result is 0.09. The correlation coefficient between $\rho_2 v_2$ and the E_y is 0.25 showing no correlation. In Figure 6b we show the density ρ_2, inflow velocity v_2, and the inflowing magnetic field B_{L2} normalized with the average value over the considered time period. The correlation between the measured reconnection rate and the magnetosheath inflow velocity is 0.69, that is, consistent with $B_{L2} v_2$ having very similar behavior as E_{pred} as expected from Ohms law, since the X line being studied is in a quasi-steady state. Correlation coefficient between E_y and B_{L2} is 0.58 showing weak correlation. The measured rate correlates well with v_2, but even better with $B_{L2} v_2$ with correlation coefficient 0.8 showing that B_{L2} affects the reconnection rate.

Figure 7 shows stacked time series of *B*, *n*, and the *x* component of the bulk velocity v_x, which can be used as an approximation of the inflow velocity, along the cut through the magnetopause at the X line location that is marked with a white line in Figure 1. Fluctuations in the magnetosheath ρ and *B* near the X line are caused by the mirror mode waves. Anticorrelation between these two parameters can still be observed near the magnetopause. Because B_{L2} had an effect on the reconnection rate and mirror modes cause the fluctuations in *B*, mirror mode waves have an effect on the measured reconnection rate. These waves propagate to the magnetopause affecting the inflow parameters. Fluctuations in the v_x seem to be independent of the mirror mode waves and are probably caused by other wave activity. Further, waves in the magnetosheath are the FTE-driven bow and stern waves that propagate in the magnetosheath from the magnetopause toward the bow shock that are discussed in the recent paper by *Pfau-Kempf* [2016]. There is also another wave activity in the magnetosheath, the study of which is outside of the scope of this work.

4. Discussion

In this paper we present the first study of the reconnection rate from a 2D-3V hybrid-Vlasov simulation of Earth's magnetosphere capable of describing ion kinetic physics globally and self-consistently. In a Vlasiator polar plane run under steady southward IMF, we observe that the reconnection is not steady; there is copious production of FTEs. Therefore, the locations of reconnection X lines vary significantly over time. Multiple X lines simultaneously exist along the magnetopause throughout the simulation, while at any given time there are only one or a few dominant X lines that are able to divert plasma flow on the magnetopause. In most cases they move away from the subsolar point toward the poles, but we also observe X lines that return back to the subsolar point after moving away from it, as has been reported before by *Sibeck and Omidi* [2012].

Observations have indicated that reconnection can occur continuously in time for several hours [*Frey et al.*, 2003; *Phan et al.*, 2004]. Our simulations show that although reconnection can occur continuously, it occurs in a dynamic nature even with steady solar wind conditions. In the subsolar region (*z* between $\pm 3\,R_E$) the

dominant X line moves significantly. Although the signatures are monitored along the magnetopause, many R_E from the X line or in the ionosphere [*Frey et al.*, 2003] may present a picture of continuous reconnection, the X line itself may be quite dynamic, even for steady IMF.

We have studied the motion of X lines at the dayside magnetopause. Previously, global magnetopause reconnection had been simulated mostly with MHD simulations. In ideal-MHD simulations with a coarse enough grid, the X line is located close to the subsolar point and reconnection attains a quasi-steady state during steady southward solar wind conditions [e.g., *Raeder*, 2006; *Hoilijoki et al.*, 2014]. We note that the X lines move more in the Vlasiator simulation under purely southward IMF than when *Hoilijoki et al.* [2014] added Parker spiral or tilted the Earth dipole in a global MHD simulation, or tilting the Earth dipole field at 20° shifted the average location of the reconnection line as much as the X lines move in the Vlasiator simulation under purely southward IMF. Using resistive-MHD simulations, *Dorelli and Bhattacharjee* [2009] showed that multiple X lines and FTEs can form in MHD simulations with a fine enough grid during steady southward IMF as well. However, MHD simulations cannot describe magnetosheath waves such as mirror mode waves. We have shown here that they can have an effect on the local reconnection rate. Therefore, adding kinetic physics in global magnetospheric modeling is important to fully describe the global effects on the local reconnection rate. Previous studies using global hybrid simulations show also that during steady southward IMF, multiple X lines exist and FTEs form [*Omidi and Sibeck*, 2007; *Sibeck and Omidi*, 2012; *Karimabadi et al.*, 2006; *Tan et al.*, 2011].

Isolated X lines drift if there is a velocity shear between the upstream regions [*Doss et al.*, 2015]. We find that the shear between the magnetospheric and magnetosheath velocities within 4 R_E of the subsolar point is small making this effect negligible. Instead, the effect of neighboring X lines dominates the X line motion. However, at higher latitudes the shear increases, along with the velocities of the X lines as they propagate toward the cusps. In general, multiple reconnection and the effect of neighboring X lines dominate near the subsolar region, while nearer the cusps the magnetosheath velocities start to play a role, as suggested by *Cowley and Owen* [1989] and *Doss et al.* [2015].

We have also studied the local reconnection rate at dayside reconnection sites. The *Cassak and Shay* [2007] formula, which has received attention as possibly describing dayside reconnection, was derived for a single nonpropagating X line assuming steady state antiparallel reconnection in a 2-D planar geometry. In our simulation there are multiple X lines reconnecting simultaneously, and reconnection at X-lines sometimes turns off as magnetic islands coalesce. In spite of this, our simulation results reveal a good correlation with the reconnection rate calculated using the analytical formula for the well-developed reconnection sites, suggesting that the local model for a single X line is still a good approximation for reconnection at the dayside magnetopause even if multiple X lines exist simultaneously. The good correlation between the measured and analytical prediction of the reconnection rate implies that the local reconnection depends on the local plasma conditions and not so much on the solar wind parameters as suggested also by *Borovsky et al.* [2008] using MHD simulations. We find that during the chosen time period the fluctuations in magnetosheath parameters are more dominant in defining the variations in the local reconnection rate being consistent with spacecraft observations by *Wang* [2015]. It is important to note, however, that here we find that the agreement with the *Cassak and Shay* [2007] analytical formula holds only if we do not assume a constant aspect ratio and use equation (2) instead (likely because of the grid resolution).

The local plasma conditions are modified by the processes upstream of the X line and by the neighboring reconnection sites at the magnetopause. Here, we find that mirror mode waves modify the local plasma parameters near the X-line, which in turn have an effect on the reconnection rates as suggested by *Laitinen et al.* [2010]. We note that the formation and propagation of magnetic islands disturb the local plasma conditions at the vicinity of the magnetopause, which influences the inflow parameters and, therefore, also reconnection rates. Propagating magnetic islands push plasma causing the X lines ahead of the islands to move; it can sometimes eventually cause them to stop reconnecting. Some X lines remain topologically as saddle points of the flux function, while the reconnection between the magnetic field lines of the Earth and magnetosheath stops and the newly reconnected field lines of the magnetic islands start to reconnect with each other. However, as the X lines are in constant motion, investigating the effect of individual factors on the reconnection rate separately is complicated.

5. Conclusions

In this paper we present the first study of the reconnection rate from a global magnetospheric 2D-3V hybrid-Vlasov simulation in the polar plane with due southward interplanetary magnetic field. We observe that even with steady southward IMF the reconnection is not steady; there are multiple X lines reconnecting simultaneously and there is copious production of FTEs. Our simulation results reveal a good correlation with the reconnection rate calculated using the *Cassak and Shay* [2007] analytical formula. The local reconnection rate depends on the local plasma conditions, which are modified by the processes upstream of the X line such as magnetosheath waves, the motion of passing magnetic islands, and the activity of the neighboring reconnection sites at the magnetopause.

Acknowledgments
The work of S.H., U.G., Y.P-K., S.V.A., and M.P. is supported by the Academy of Finland (SA-Vlasov grant 267144) and ERC consolidator grant ERC-CoG-682068-PRESTISSIMO. The work of P.A.C. is supported by NSF grant AGS-0953463, and NASA grants NNX16AF75G and NNX16AG76G. B.M.W. is supported by NASA grants NNX16AD91G and NNX16AJ73G. H.H. is supported by NASA contract NAS5-02099. The run was carried out using HLRS/Stuttgart Hazel Hen through PRACE Tier-0 resource grant (2014112573) from the 12th call. Data shown in this paper can be accessed by following the data policy on our web page http://vlasiator.fmi.fi/rules.php.

References

Birn, J., J. E. Borovsky, M. Hesse, and K. Schindler (2010), Scaling of asymmetric reconnection in compressible plasmas, *Phys. Plasmas*, *17*(5), 052108, doi:10.1063/1.3429676.

Blanco-Cano, X., N. Omidi, and C. Russell (2006), ULF waves and their influence on bow shock and magnetosheath structures, *Adv. Space Res.*, *37*(8), 1522–1531, doi:10.1016/j.asr.2005.10.043.

Blanco-Cano, X., N. Omidi, and C. T. Russell (2009), Global hybrid simulations: Foreshock waves and cavitons under radial interplanetary magnetic field geometry, *J. Geophys. Res.*, *114*, A01216, doi:10.1029/2008JA013406.

Borovsky, J. E., M. Hesse, J. Birn, and M. M. Kuznetsova (2008), What determines the reconnection rate at the dayside magnetosphere?, *J. Geophys. Res.*, *113*, A07210, doi:10.1029/2007JA012645.

Cassak, P. A., and A. Otto (2011), Scaling of the magnetic reconnection rate with symmetric shear flow, *Phys. Plasmas*, *18*(7), 074501, doi:10.1063/1.3609771.

Cassak, P. A., and M. A. Shay (2007), Scaling of asymmetric magnetic reconnection: General theory and collisional simulations, *Phys. Plasmas*, *14*(10), 102114, doi:10.1063/1.2795630.

Cassak, P. A., and M. A. Shay (2009), Response to comment on scaling of asymmetric magnetic reconnection: General theory and collisional simulations, *Phys. Plasmas*, *16*(3), 034702, doi:10.1063/1.3083264.

Chen, Q., A. Otto, and L. C. Lee (1997), Tearing instability, Kelvin-Helmholtz instability, and magnetic reconnection, *J. Geophys. Res.*, *102*, 151–162, doi:10.1029/96JA03144.

Cowley, S. W. H., and C. J. Owen (1989), A simple illustrative model of open flux tube motion over the dayside magnetopause, *Planet. Space Sci.*, *37*, 1461–1475, doi:10.1016/0032-0633(89)90116-5.

Daldorff, L. K., G. Tóth, T. I. Gombosi, G. Lapenta, J. Amaya, S. Markidis, and J. U. Brackbill (2014), Two-way coupling of a global hall magnetohydrodynamics model with a local implicit particle-in-cell model, *J. Comput. Phys.*, *268*, 236–254, doi:10.1016/j.jcp.2014.03.009.

Dorelli, J. C., and A. Bhattacharjee (2009), On the generation and topology of flux transfer events, *J. Geophys. Res.*, *114*, A06213, doi:10.1029/2008JA013410.

Doss, C. E., C. M. Komar, P. A. Cassak, F. D. Wilder, S. Eriksson, and J. F. Drake (2015), Asymmetric magnetic reconnection with a flow shear and applications to the magnetopause, *J. Geophys. Res. Space Physics*, *120*, 7748–7763, doi:10.1002/2015JA021489.

Dungey, J. W. (1953), The motion of magnetic fields, *Mon. Not. R. Astron. Soc.*, *113*, 679–682, doi:10.1093/mnras/113.6.679.

Dungey, J. W. (1961), Interplanetary magnetic field and the auroral zones, *Phys. Rev. Lett.*, *6*, 47–48, doi:10.1103/PhysRevLett.6.47.

Eastwood, J. P., T. D. Phan, R. C. Fear, D. G. Sibeck, V. Angelopoulos, M. Øieroset, and M. A. Shay (2012), Survival of flux transfer event (FTE) flux ropes far along the tail magnetopause, *J. Geophys. Res.*, *117*, A08222, doi:10.1029/2012JA017722.

Fear, R. C., S. E. Milan, A. N. Fazakerley, K.-H. Fornaçon, C. M. Carr, and I. Dandouras (2009), Simultaneous observations of flux transfer events by THEMIS, Cluster, Double Star, and SuperDARN: Acceleration of FTEs, *J. Geophys. Res.*, *114*, A10213, doi:10.1029/2009JA014310.

Fear, R. C., S. E. Milan, J. Raeder, and D. G. Sibeck (2010), Asymmetry in the bipolar signatures of flux transfer events, *J. Geophys. Res.*, *115*, A11217, doi:10.1029/2010JA015363.

Fedder, J. A., S. P. Slinker, J. G. Lyon, and C. T. Russell (2002), Flux transfer events in global numerical simulations of the magnetosphere, *J. Geophys. Res.*, *107*, 1048, doi:10.1029/2001JA000025.

Frey, H. U., T. D. Phan, S. A. Fuselier, and S. B. Mende (2003), Continuous magnetic reconnection at Earth's magnetopause, *Nature*, *426*, 533–537.

Génot, V., E. Budnik, P. Hellinger, T. Passot, G. Belmont, P. M. Trávníček, P.-L. Sulem, E. Lucek, and I. Dandouras (2009), Mirror structures above and below the linear instability threshold: Cluster observations, fluid model and hybrid simulations, *Ann. Geophys.*, *27*, 601–615, doi:10.5194/angeo-27-601-2009.

Génot, V., L. Broussillou, E. Budnik, P. Hellinger, P. M. Trávníček, E. Lucek, and I. Dandouras (2011), Timing mirror structures observed by Cluster with a magnetosheath flow model, *Ann. Geophys.*, *29*(10), 1849–1860, doi:10.5194/angeo-29-1849-2011.

Hoilijoki, S., V. M. Souza, B. M. Walsh, P. Janhunen, and M. Palmroth (2014), Magnetopause reconnection and energy conversion as influenced by the dipole tilt and the IMF B_x, *J. Geophys. Res. Space Physics*, *119*, 4484–4494, doi:10.1002/2013JA019693.

Hoilijoki, S., M. Palmroth, B. M. Walsh, Y. Pfau-Kempf, S. V. Alfthan, U. Ganse, O. Hannuksela, and R. Vainio (2016), Mirror modes in the Earth's magnetosheath: Results from a global hybrid-Vlasov simulations, *J. Geophys. Res. Space Physics*, *121*, 4191–4204, doi:10.1002/2015JA022026.

Karimabadi, H., H. X. Vu, D. Krauss-Varban, and Y. Omelchenko (2006), Global hybrid simulations of the Earth's magnetosphere, in *Numerical Modeling of Space Plasma Flows*, vol. 359, edited by G. P. Zank, pp. 257, Astronomical Society of the Pacific Conference Series, Palm Springs, Calif.

Karimabadi, H., et al. (2014), The link between shocks, turbulence, and magnetic reconnection in collisionless plasmas, *Phys. Plasmas*, *21*(6), 062308, doi:10.1063/1.4882875.

Kawano, H., and C. T. Russell (1997), Survey of flux transfer events observed with the ISEE 1 spacecraft: Dependence on the interplanetary magnetic field, *J. Geophys. Res.*, *102*, 11,307–11,314, doi:10.1029/97JA00481.

Kempf, Y., D. Pokhotelov, O. Gutynska, L. B. Wilson III, B. M. Walsh, S. V. Alfthan, O. Hannuksela, D. G. Sibeck, and M. Palmroth (2015), Ion distributions in the Earth's foreshock: Hybrid-Vlasov simulation and THEMIS observations, *J. Geophys. Res. Space Physics*, *120*, 3684–3701, doi:10.1002/2014JA020519.

Komar, C. M., and P. A. Cassak (2016), The local dayside reconnection rate for oblique interplanetary magnetic fields, *J. Geophys. Res. Space Physics*, *121*(6), 5105–5120, doi:10.1002/2016JA022530.

La BelleHamer, A. L., A. Otto, and L. C. Lee (1994), Magnetic reconnection in the presence of sheared plasma flow: Intermediate shock formation, *Phys. Plasmas*, *1*(3), 706–713, doi:10.1063/1.870816.
Laitinen, T. V., Y. V. Khotyaintsev, M. André, A. Vaivads, and H. Rème (2010), Local influence of magnetosheath plasma beta fluctuations on magnetopause reconnection, *Ann. Geophys.*, *28*(5), 1053–1063, doi:10.5194/angeo-28-1053-2010.
Lee, L. C., and Z. F. Fu (1985), A theory of magnetic flux transfer at the Earth's magnetopause, *Geophys. Res. Lett.*, *12*, 105–108, doi:10.1029/GL012i002p00105.
Li, J. H., and Z. W. Ma (2010), Nonlinear evolution of resistive tearing mode with sub-Alfvenic shear flow, *J. Geophys. Res.*, *115*, A09216, doi:10.1029/2010JA015315.
Mitchell Jr., H. G., and J. R. Kan (1978), Merging of magnetic fields with field-aligned plasma flow components, *J. Plasma Phys.*, *20*, 31–45, doi:10.1017/S0022377800021346.
Murphy, N. A., C. R. Sovinec, and P. A. Cassak (2010), Magnetic reconnection with asymmetry in the outflow direction, *J. Geophys. Res. Space Physics*, *115*, A09206, doi:10.1029/2009JA015183.
Omidi, N., and D. G. Sibeck (2007), Flux transfer events in the cusp, *Geophys. Res. Lett.*, *34*, L04106, doi:10.1029/2006GL028698.
Ouellette, J. E., J. G. Lyon, and B. N. Rogers (2014), A study of asymmetric reconnection scaling in the Lyon-Fedder-Mobarry code, *J. Geophys. Res. Space Physics*, *119*, 1673–1682, doi:10.1002/2013JA019366.
Palmroth, M., et al. (2015), ULF foreshock under radial IMF: THEMIS observations and global kinetic simulation Vlasiator results compared, *J. Geophys. Res. Space Physics*, *120*, 8782–8798, doi:10.1002/2015JA021526.
Pfau-Kempf, Y., H. Hietala, S. E. Milan, L. Juusola, S. Hoilijoki, U. Ganse, S. von Alfthan, and M. Palmroth (2016), Evidence for transient, local ion foreshocks caused by dayside magnetopause reconnection, *Ann. Geophys.*, *34*(11), 943–959, doi:10.5194/angeo34-943-2016.
Phan, T., et al. (2004), Cluster observations of continuous reconnection at the magnetopause under steady interplanetary magnetic field conditions, *Ann. Geophys.*, *22*, 2355–2367, doi:10.5194/angeo-22-2355-2004.
Raeder, J. (2006), Flux transfer events: 1. Generation mechanism for strong southward IMF, *Ann. Geophys.*, *24*(1), 381–392, doi:10.5194/angeo-24-381-2006.
Rijnbeek, R. P., Cowley, S. W. H., Southwood, D. J., and C. T. Russell (1984), A survey of dayside flux transfer events observed by ISEE 1 and 2 magnetometers, *J. Geophys. Res.*, *89*, 786–800, doi:10.1029/JA089iA02p00786.
Russell, C., G. Le, and H. Kuo (1996), The occurrence rate of flux transfer events, *Adv. Space Res.*, *18*(8), 197–205, doi:10.1016/0273-1177(95)00965-5.
Russell, C. T., and R. C. Elphic (1978), Initial ISEE magnetometer results—Magnetopause observations, *Space Sci. Rev.*, *22*, 681–715, doi:10.1007/BF00212619.
Scholer, M. (1988), Magnetic flux transfer at the magnetopause based on single X line bursty reconnection, *Geophys. Res. Lett.*, *15*, 291–294, doi:10.1029/GL015i004p00291.
Servidio, S., W. H. Matthaeus, M. A. Shay, P. A. Cassak, and P. Dmitruk (2009), Magnetic reconnection in two-dimensional magnetohydrodynamic turbulence, *Phys. Rev. Lett.*, *102*, 115,003, doi:10.1103/PhysRevLett.102.115003.
Servidio, S., W. H. Matthaeus, M. A. Shay, P. Dmitruk, P. A. Cassak, and M. Wan (2010), Statistics of magnetic reconnection in two-dimensional magnetohydrodynamic turbulence, *Phys. Plasmas*, *17*(3), 032,315, doi:10.1063/1.3368798.
Shi, Y., C. C. Wu, and L. C. Lee (1988), A study of multiple X line reconnection at the dayside magnetopause, *Geophys. Res. Lett.*, *15*, 295–298, doi:10.1029/GL015i004p00295.
Sibeck, D. G., and N. Omidi (2012), Flux transfer events: Motion and signatures, *J. Atmos. Sol. Terr. Phys.*, *87*, 20–24, doi:10.1016/j.jastp.2011.07.010.
Southwood, D., C. Farrugia, and M. Saunders (1988), What are flux transfer events?, *Planet. Space Sci.*, *36*(5), 503–508, doi:10.1016/0032-0633(88)90109-2.
Tan, B., Y. Lin, J. D. Perez, and X. Y. Wang (2011), Global-scale hybrid simulation of dayside magnetic reconnection under southward IMF: Structure and evolution of reconnection, *J. Geophys. Res.*, *116*(A2), A02206, doi:10.1029/2010JA015580.
Tátrallyay, M., and G. Erdős (2005), Statistical investigation of mirror type magneticfield depressions observed by ISEE-1, *Planet. Space Sci.*, *53*, 33–40, doi:10.1016/j.pss.2004.09.026.
von Alfthan, S., D. Pokhotelov, Y. Kempf, S. Hoilijoki, I. Honkonen, A. Sandroos, and M. Palmroth (2014), Vlasiator: First global hybrid-Vlasov simulations of Earth's foreshock and magnetosheath, *J. Atmos. Sol. Terr. Phys.*, *120*, 24–35, doi:10.1016/j.jastp.2014.08.012.
Wang, Y. L., et al. (2005), Initial results of high-latitude magnetopause and low-latitude flank flux transfer events from 3 years of Cluster observations, *J. Geophys. Res.*, *110*, A11221, doi:10.1029/2005JA011150.
Wang, S., L. M. Kistler, C. G. Mouikis, and S. M. Petrinec (2015), Dependence of the dayside magnetopause reconnection rate on local conditions, *J. Geophys. Res. Space Physics*, *120*, 6386–6408, doi:10.1002/2015JA021524.
Wang, Y. L., R. C. Elphic, B. Lavraud, M. G. G. T. Taylor, J. Birn, C. T. Russell, J. Raeder, H. Kawano, and X. X. Zhang (2006), Dependence of flux transfer events on solar wind conditions from 3 years of Cluster observations, *J. Geophys. Res.*, *111*, A04224, doi:10.1029/2005JA011342.
Yeates, A. R., and G. Hornig (2011), A generalized flux function for three-dimensional magnetic reconnection, *Phys. Plasmas*, *18*(10), 102118, doi:10.1063/1.3657424.